Elastic metamaterials with inertial locally resonant structures: Application to lensing and localization

D. Bigoni,[1] S. Guenneau,[2,*] A. B. Movchan,[3] and M. Brun[3,4]

[1]*Department of Civil, Environmental and Mechanical Engineering, University of Trento, Via Mesiano 77, I-38050 Trento, Italy*

[2]*Aix-Marseille Université, CNRS, Ecole Centrale Marseille, Institut Fresnel, 13013 Marseille, France*

[3]*Department of Mathematical Sciences, Peach Street, The University of Liverpool, Liverpool, L69 3BX, United Kingdom*

[4]*Dipartimento di Ingegneria Meccanica, Chimica e dei Materiali, Universitá di Cagliari, Piazza d'Armi, Cagliari I-09123, Italy*

(Received 23 December 2012; revised manuscript received 28 April 2013; published 29 May 2013)

We propose a type of locally resonant structure involving arrays of structured coated inclusions. The coating consists of a structural interface with beams inclined at a certain angle. Such an elastic metamaterial supports tunable low-frequency stop bands associated with localized rotational modes that can be used in the design of filtering, reflecting, and focusing devices. Asymptotic estimates for resonant frequencies are in good agreement with finite element computations and can be used as a design tool to tune stop band changing relative inclinations, number, and cross section of the beams. Inertial resonators with inclined ligaments allow for anomalous dispersion (negative group velocity) to occur in the pressure acoustic band and this leads to the physics of negative refraction, whereby a point force located above a finite array of resonators is imaged underneath for a given polarization. We finally observe that for a periodic macrocell of the former inertial resonators with one defect in the middle, an elastic trapped mode exists within a high-frequency stop band. The latter design could be used in the enhancement of light and sound interactions in photonic crystal fiber preforms.

DOI: 10.1103/PhysRevB.87.174303 PACS number(s): 47.65.−d, 47.35.Lf, 47.11.Fg, 47.11.St

I. INTRODUCTION

The work by Nicorovici *et al.* (1994)[1] has developed an analytical model analyzing optical and dielectric properties of partially resonant systems. This was highly significant conceptual work, which paved the way towards modeling of metamaterial systems. In particular, Nicorovici and Milton (2006)[2] have explained important cloaking effects based on the anomalous localized resonances. The work by Veselago (1968)[3] has provided motivation and stimulated development of analysis towards structures possessing the property of negative refraction. Following the idea of Pendry *et al.* (1999)[4] of split-ring resonators and implementation of the negative refraction system by Smith *et al.* (2000),[5] Movchan and Guenneau (2004)[6] and Guenneau *et al.* (2007)[7] used an asymptotic approach for a system of multiscale split-ring resonators to evaluate the low frequencies of standing waves and the boundaries of stop bands, which had given a simple way to an optimal design of a multiscale metamaterial system. Furthermore, Brun *et al.* (2010a, 2010b)[8,9] in different configurations involving a formulation for elastic waves interacting with a structured interface identified resonance trapped modes linked to high Q-factor transmission resonances across the structured interface.

Liu *et al.* (2000) provided numerical and experimental demonstrations of locally resonant structures for elastic waves in 3D arrays of thin coated spheres.[10] This work was useful for acoustic analogs of electromagnetic metamaterials, such as fluid-solid composites.[11] Li and Chan independently proposed a similar type of negative acoustic metamaterial.[12] In a recent work, Fang *et al.* experimentally demonstrated a dynamic effective negative stiffness in a chain of water-filled Helmholtz resonators for ultrasonic waves.[13]

In 2006, Milton, Briane, and Willis provided a thorough mathematical frame for such effects including cloaking for elastodynamic waves,[14] shown numerically for an annular cloak in Ref. 15 with an alternative model. Milton and Norris independently furthered the theory of acoustic cloaking analyzing the underlying continuum elastodynamic governing equations.[16,17] Such neutral inclusions have also been studied in the elastostatic context using asymptotic and computational methods in the case of antiplane shear and in-plane coupled pressure and shear polarizations.[18]

Cummer and Schurig demonstrated that acoustic waves in a fluid also undergo the same geometric transform for a 2D geometry,[19] which has been since then generalized to 3D acoustic cloaks for pressure waves.[20,21] Such cloaks require an anisotropic mass density unlike the acoustic cloak for linear surface water waves studied experimentally and theoretically in Ref. 22. Demonstration of a design of a focusing flat lense via negative refraction for surface water waves has been published in Refs. 23–25 and focusing in a 3D phononic crystal was modeled in Ref. 26. The extension of these phenomena to the area of in-plane elastodynamic waves is a further challenge, with some recent advances[27–30] including a first design of a convergent flat lens using structural interfaces in Ref. 9. Interestingly, achieving focusing of flexural waves in perforated elastic plates is far less challenging.[31]

Cellular lattice structures with low natural frequency were introduced in Refs. 32 and 33, inspired by the molecular model described by Wojciechowski.[34] Their static and dynamic behavior was successively analyzed in Refs. 35 and 36. In such lattice structures the Lamé constants and the density are of several orders of magnitude smaller than the corresponding physical quantities of the constituent material composing the microstructure. As detailed in Ref. 32 applications in packaging, low-density cores, filters, and insulation depend on the quasistatic properties of these materials and hence would significantly change with the alteration of volume fraction of a periodic system.

In the present paper, we propose a structured medium where the average mass density and the elastic constants are of the same order as the constituent material, and where a periodic system of torsional resonators can be tuned to achieve low-frequency standing waves and stop bands. We also show that it is possible to design some tunable locally resonant metamaterial for in-plane elastic waves which serves two purposes: focusing flat lens and defect localization for low-frequency phononic band gap guidance. We demonstrate theoretically their mechanism and further perform finite element computations checked against asymptotic formulas. Potential applications are in medical imaging and photonic fiber preforms for optoacoustic switches via Brillouin scattering,[37,38] but also in passive anti-earthquake systems (thanks to low-frequency elastic stop bands).

II. SETUP OF THE SPECTRAL PROBLEM

Time-harmonic propagation of in-plane elastic waves is considered. The equations of motion are expressed in term of the displacement field $\mathbf{u}(\mathbf{x},t) = \mathbf{U}(\mathbf{x})e^{i\omega t}$ in the point $\mathbf{x} = (x_1,x_2)$ at time t where ω is the radian frequency and $\mathbf{u} = (u_1,u_2)$, $\mathbf{U} = (U_1,U_2)$. The vector Navier equations can be expressed in the form

$$\hat{\mu}(\mathbf{x})\nabla^2\mathbf{U} + [\hat{\lambda}(\mathbf{x}) + \hat{\mu}(\mathbf{x})]\nabla(\nabla\cdot\mathbf{U}) + \hat{\rho}(\mathbf{x})\omega^2\mathbf{U} = \mathbf{0}, \qquad (1)$$

with density $\hat{\rho}(\mathbf{x}) = \chi^{(r)}(\mathbf{x})\rho^{(r)}$ and Lamé constants $\hat{\lambda}(\mathbf{x}) = \chi^{(r)}(\mathbf{x})\lambda^{(r)}$, $\hat{\mu}(\mathbf{x}) = \chi^{(r)}(\mathbf{x})\mu^{(r)}$, where $\chi^{(r)}(\mathbf{x})$ is the indicator function which is equal to 1 in phase r and 0 otherwise and $\lambda^{(r)}$, $\mu^{(r)}$, and $\rho^{(r)}$ the material parameters in the phase r.

The elementary cell of the periodic structure includes a void containing a resonator as shown in Fig. 1. The resonator consists of a core region at the center and uniformly distributed thin ligaments. It is noted that the orientation of ligaments is not radial, and hence rotation of the core region leads to compressive or tensile radial stress on the boundary of the void. In other words, such a system provides a coupling between shear (due to rotation) and pressure (due to radial stress) at the boundary of the void.

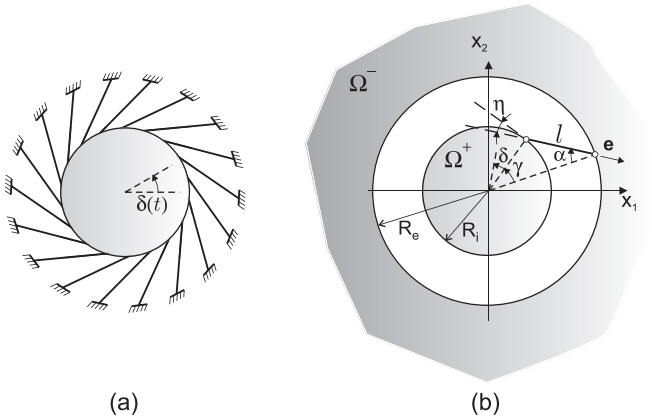

FIG. 1. Structural interface for a circular inclusion Ω^+ in a continuum medium Ω^-. The beams have length $l = \sqrt{R_i^2 + R_e^2 - 2R_eR_i\cos\gamma}$, thickness s, and relative inclination $\eta = \pi/2 - \gamma - \alpha$. (a) Simplified model for the asymptotic approximation. (b) Detail of the geometrical parameters.

We are looking for real positive eigenfrequencies ω associated with nontrivial solutions of (1) in the class of Floquet-Bloch vector valued functions

$$\mathbf{U}(x_1 + md, x_2 + nd) = \mathbf{U}(x_1,x_2)e^{i(k_1md+k_2nd)}, \qquad (2)$$

where $\mathbf{k} = (k_1,k_2)^T$ is the so-called Bloch vector describing the first Brillouin zone $Y^* = [-\pi/d,\pi/d]^2$, counterpart of the basic cell $Y = [-d,d]^2$ in the reciprocal space. Moreover, m and n are integers indexing a node of the lattice in reciprocal space, and d is the pitch of the array in physical space. We note that Y^* can be reduced to the right-angled triangle ΓMX with vertices $\Gamma = (0,0)$, $M = (\pi/d,0)$, and $X = (\pi/d,\pi/d)$, if the geometry of the problem is fourfold (as in the present case).

The paper presents an outline of the dynamic coupling between shear and pressure in the boundary conditions. It is noted that the orientation of the inclination of the ligaments within the interface affects the direction of rotation of the core region and hence the coupling between the shear and pressure waves. Furthermore, the numerical model is developed to analyze the dispersion of coupled in-plane pressure and shear waves propagating within an array of inclusions.

III. ASYMPTOTIC ESTIMATES FOR A SINGLE RESONATOR

The inertial resonator is shown in Fig. 1. For convenience, we assume that the inclusion at the center is taken as rigid and the N inclined connecting bars are elastic massless beams or trusses. The geometrical parameters are shown in Fig. 1(b).

We are concerned with a class of standing waves in a periodic system containing inclusions with the structured coating. The vibration modes in this simplified mechanical model are obtained via the introduction of the rotation angle $\delta(t)$. Let u_r and u_δ denote the radial and tangential displacements on the contour of the void. Direct derivation shows that the rotational motion of the core region is governed by the differential equation

$$\ddot{\delta} + \omega_0^2\delta = \frac{\omega_0^2}{R_i\cos\eta}(u_\delta\sin\alpha - u_r\cos\alpha), \qquad (3)$$

with geometrical parameters α, η, and R_i defined in Fig. 1(b) and vibration frequency

$$\omega_0 = \sqrt{2\kappa/M}\cos\eta. \qquad (4)$$

Here M is the mass of the central core region, $\kappa = EA/l$ is the total longitudinal stiffness of inclined bars, E is Young's modulus, l is the beam length, and $A = NA_s$ is the total cross-sectional area of the N bars with the cross section A_s and thickness s. We note that ω_0 vanishes when the connecting bars become radial, which corresponds to the degenerate case, where flexural deformation of the bars has to be taken into account, and the eigenfrequency of the corresponding vibration mode is substantially reduced.

Direct calculations show that the averaged tractions t_n and t_δ on the contour of the void are given by

$$t_n = \frac{\kappa\delta R_i\cos\eta\cos\alpha}{2\pi R_e}, \quad t_\delta = -\frac{\kappa\delta R_i\cos\eta\sin\alpha}{2\pi R_e}, \qquad (5)$$

and hence the coupling between the tangential and normal tractions is defined as

$$t_\delta = -t_n \tan\alpha, \tag{6}$$

where $\alpha \neq 0$ for the nondegenerate interface with inclined bars. A resonance mode, corresponding to the case when $\omega \to \omega_0$, is of special interest. In this case, the function $\delta(t)$ satisfies $\ddot{\delta} + \omega_0^2\delta = 0$, and hence the displacements on the contour of the void are related by

$$u_\delta \tan\alpha = u_r. \tag{7}$$

Equation (3) shows the coupling between the radial compression/extension along the boundary of the void and the rotation of the central core. In the special case of the radially symmetric resonance mode of frequency ω_0, the effective boundary conditions, which show coupling between the shear and tensile deformations on the contour of the void, are given by (6) and (7). The above deductions are applicable for the nondegenerate case, when $\alpha \neq 0$, and they fail otherwise.

When the system in Fig. 1 degenerates, as $\alpha \to 0$, the flexural deformations of the connecting beams have to be taken into account in order to evaluate the resonance frequency of the resonator. In the corresponding asymptotic approximation of the first eigenfrequency, it is feasible to assume the circular contour as rigid, as shown in Fig. 1(a). The kinetic energy of this mechanical system is

$$\mathcal{K}(t) = \frac{1}{2}\frac{M R_i^2}{2}\dot{\delta}^2(t), \tag{8}$$

whereas the potential energy, referred to the structured beam interface only, is

$$\mathcal{P}(t) = \frac{1}{2}\kappa\left[R_i^2\cos^2\eta + \frac{s^2}{3l^2}\left(3R_i^2\sin^2\eta + 3R_i l\sin\eta + l^2\right)\right] \times \delta^2(t). \tag{9}$$

Then, the Euler-Lagrange equation, deduced from Eqs. (8) and (9), corresponds to the balance of angular momentum for the rigid inclusion, and it takes the form

$$\frac{M R_i^2}{2}\ddot{\delta(t)} + \kappa\left[R_i^2\cos^2\eta + \frac{s^2}{3l^2}\left(3R_i^2\sin^2\eta + 3R_i l\sin\eta + l^2\right)\right]\delta(t) = 0. \tag{10}$$

Under the assumption $\delta(t) = \Delta e^{i\omega t}$ the natural frequency ω_0 of the system in Fig. 1(a) is

$$\omega_0 = \sqrt{\cos^2\eta + \frac{s^2}{3l^2}\left(3\sin^2\eta + 3\frac{l}{R_i}\sin\eta + \frac{l^2}{R_i^2}\right)}\sqrt{\frac{2\kappa}{M}}. \tag{11}$$

The eigenfrequencies, estimated in (4) and (11), can be efficiently tuned by changing geometric and material parameters of the composite, such as relative inclinations, number, and cross section of the beams. We shall see in the sequel that the asymptotic estimate (11) predicts with a good accuracy the frequency corresponding to a localized rotational mode within a square array of inertial resonators (IRs).

Although the formulas (4) and (11) are derived on the basis of an asymptotic model of a single resonator, this is exactly what is required for analysis of a standing wave on an elementary cell of a doubly periodic structure. The vibration modes for such a standing wave are localized, so that on the boundary of the elementary cell of periodicity the amplitude of displacements is negligibly small compared to the displacement amplitude within the rotational resonator.

IV. NUMERICAL SIMULATIONS

We now investigate numerically the stop band properties of a periodic structure consisting of inertial resonators (IRs) when the beams make either a large or a small angle with the normal to their circular boundaries. We shall see that in the former case the lowest resonance of IRs induces a nearly flat band in the high-frequency range (Bragg regime), so that the array can be considered as a bare phononic crystal. However, in the latter case the lowest resonance of IRs opens a low-frequency stop band in a way similar to what split ring resonators achieve for electromagnetic and acoustic waves in metamaterials.

Stop bands for arrays of inertial resonators. Let us first look at the case of a structure with voids shaped as shown in Fig. 2(b). For convenience, we use the normalized Lamé constants $\lambda = 2.3$, $\mu = 1$, which correspond to a Poisson ratio $\nu = 0.3485$ common for many elastic materials, a Young's to shear modulus ratio $E/\mu = 2.6966$, a density $\rho = 1$, so that the shear wave speed is $v_s = \sqrt{\mu/\rho} = 1$. We notice the presence in Fig. 2(a) of a nearly flat dispersion curve (depicted in light gray dashed line) for which the the group velocity $\partial\omega/\partial\mathbf{k}$ vanishes: This is a standing wave of normalized frequency $\omega_r = \omega d/v_s = 3.59$ for $\mathbf{k} = (0,0)$ and $\omega_r = 3.61$ for $\mathbf{k} = (\pi,\pi)$, with $d/v_s = 1$. The associated eigenfield is of rotational nature, as can be seen from right panel of Fig. 2. The frequency estimate deduced from Eq. (4) leads to the value $\omega_0 \sim 3.78$ since $\eta = \pi/3$; the total longitudinal stiffness of inclined bars is $\kappa = 2.6966 \times 8 \times 0.05/0.3\,\mu = 3.5954\,\mu$ and $M = \pi\,0.2^2\,\rho = 0.1257\,\mu$. This localized mode occurs at a frequency within the stop band corresponding to a doubly periodic array (of period d) of voids of radius $R_e = 0.4$.

We now want to tune down the stop band of the metamaterial. For this, we consider a small inclination of the ligaments (i.e., beams) within the inertial resonators. We observe a rotational mode at normalized frequency $\omega_r = 2.60$. The frequency estimate deduced from Eq. (11) leads to the value $\omega_0 \sim 2.77$, since $\eta = 14\pi/30$, $s/R_i = 0.25$, $l/R_i = 1.3$; the total longitudinal stiffness is $\kappa = 2.6966 \times 0.05 \times 8/0.26\,\mu = 4.1486\,\mu$ as bars are now less inclined and $M = 0.1257\,\mu$. We note that this localized mode occurs at a frequency below the stop band observed for the doubly periodic system with voids of radius $R_e = 0.4$. These results are reported in Fig. 3, where it should be noted that the matrix material surrounding the inertial resonator is subjected to displacements of negligible magnitude with respect to the inclusion and the ligaments.

Compared to the lattice system in Refs. 35 and 36, where the effective Poisson's ratio is negative and the effective group velocities of pressure and shear waves are close to each other in the long-wave limit, our system represents the full vector problem of elasticity where both shear and pressure wave propagate within the medium with distinctively different velocities. The frequency discussed in the text is rightly in the

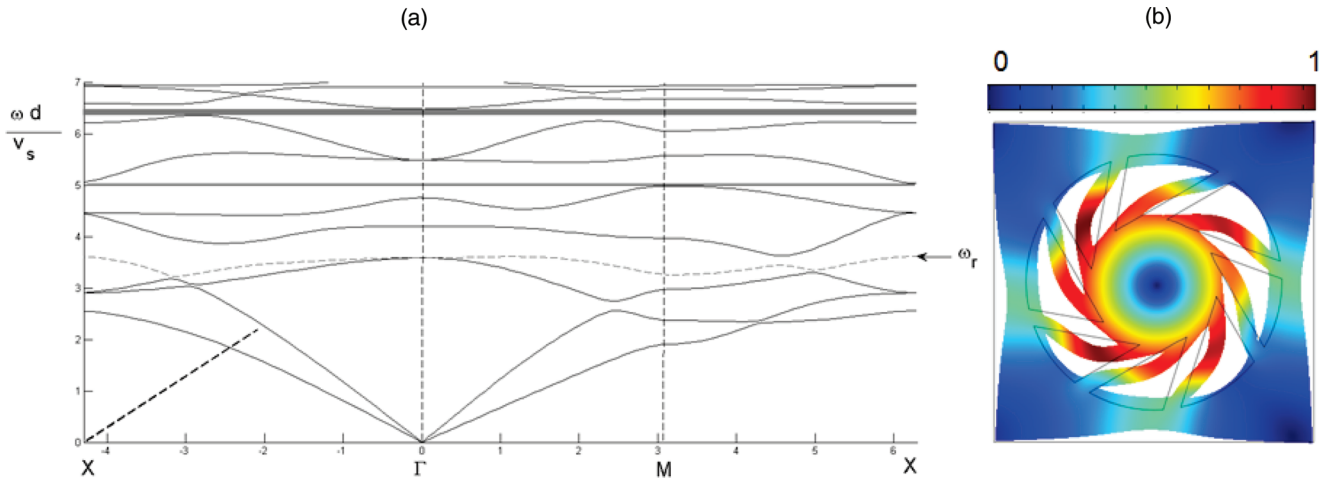

FIG. 2. (Color online) (a) Band diagram for a square array of inclusions (core of radius $R_i = 0.2$ and outer interface of radius $R_e = 0.4$) with eight most inclined ligaments. (b) Deformation of the elastic unit cell for the fourth eigenmode (cf. light gray dashed curve on left diagram) when the Bloch vector is $\mathbf{k} = (\pi,\pi)$. Color map indicates displacement magnitude. The rotational nature of the mode is noted, and its normalized frequency $\omega_r = \omega d/v_s = 3.71$ (d is the pitch of the array and v_s the shear wave speed) for a Bloch vector $\mathbf{k} = (\pi,\pi)$. The rotational frequency predicted by the asymptotic estimate (4) is $\omega_r = 3.78$. The lower edge of the first stop band is a nearly flat curve (light gray dashed curve) which corresponds to the frequency of the localized rotational mode. The next two stop bands are shown in gray color. The blue dotted line corresponds to the shear waves in a homogeneous isotropic medium and its intersection with the first acoustic band gives the frequency at which all-angle-negative refraction occurs.

range of interest. This frequency can be reduced further by increase of the mass of the resonator core or decrease of the stiffness of elastic ligaments, if required. We also mention that our focus is on the nondegenerate case where ligaments are not radial and the frequency is expected to be higher. When the ligaments become radial the rotational mode will become degenerate, which would lead to a significant reduction of the frequency of the angular motion.

Elastic trapped mode in a macrocell with defect. Let us analyze a periodic macrocell consisting of 24 inclusions arranged as in Fig. 4: This corresponds to a doubly periodic array of defects (obtained through the removal of an inertial resonator within a macrocell). We look at the case of IR with most inclined beams; see Fig. 4. We find a defect mode in the tiny stop band $\omega_r \in [3.68,3.82]$ whose lower edge is the light gray dashed curve in Fig. 2. This trapped mode at frequency $\omega_r = 3.71$ is of predominant dilatational nature. The next trapped mode occurs for $\omega_r = 5.05$, that is in the second stop band $\omega_r \in [4.95,5.09]$ shown in gray in Fig. 2. This trapped mode is also of predominant dilatational nature.

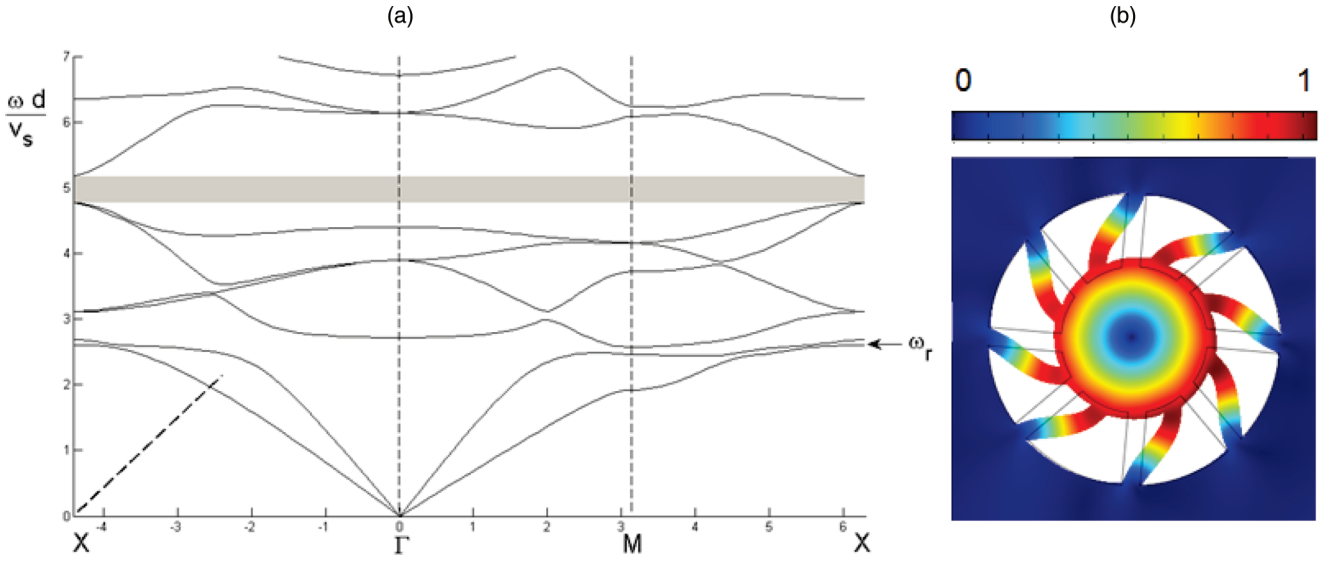

FIG. 3. (Color online) Same as in Fig. 2 but for eight slightly inclined ligaments. Color map indicates displacement magnitude. The rotational nature of the mode is noted in panel (b), and its normalized frequency $\omega_r = 2.60$ for a Bloch vector $\mathbf{k} = (\pi,\pi)$. The rotational frequency predicted by the asymptotic estimate (11) is 2.77. This mode creates a low-frequency stop band within which negative refraction occurs.

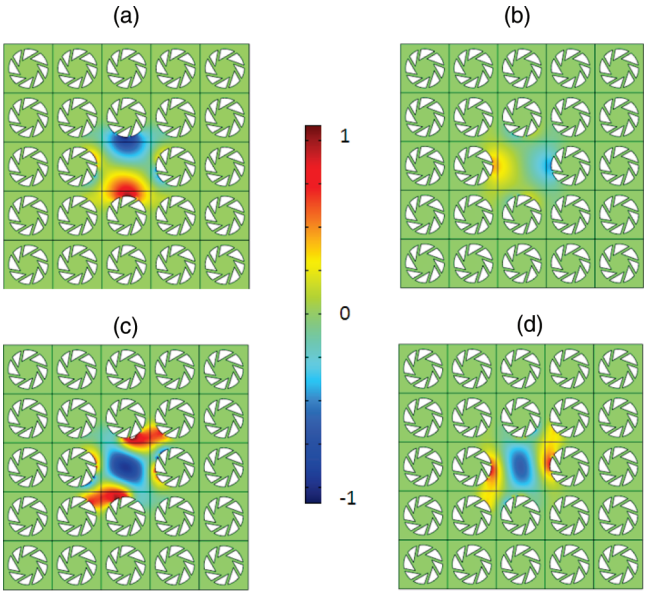

FIG. 4. (Color online) Macrocell consisting of 24 inclusions as in Fig. 2, whereby the central inclusion has been removed, leading to trapped modes associated with flat dispersion curves in the stop bands of the periodic structure. The first two trapped modes belong respectively to the stop band whose lower edge corresponds to the red curve and to the tiny stop band shown in gray in Fig. 2. (a), (c) Dilatational component $\partial u_1/\partial x_1 + \partial u_2/\partial x_2$ for a trapped mode at frequency $\omega d/v_s = 3.71$ (a) and 5.05 (c). (b), (d) Shear component $0.5(\partial u_1/\partial x_2 + \partial u_2/\partial x_1)$ of the trapped modes at frequency $\omega d/v_s = 3.71$ (b) and 5.05 (d). We note that the two trapped modes have a predominant dilatation component.

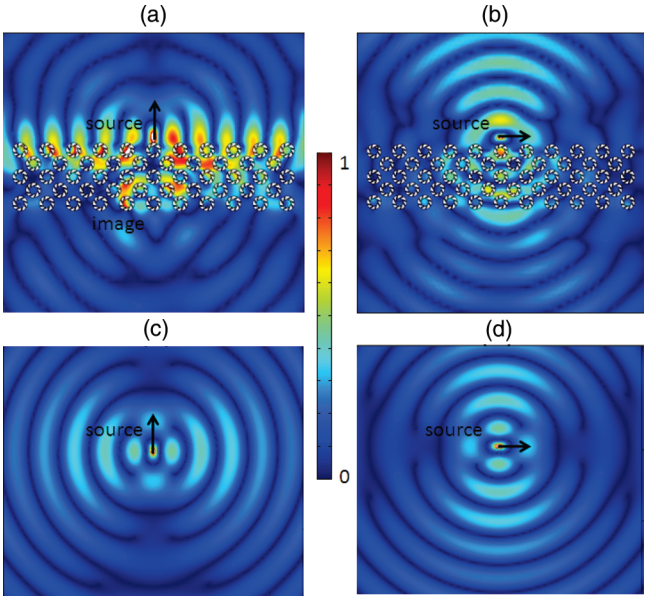

FIG. 5. (Color online) Plot of the magnitude of displacement field for a point force of polarization (1,0) [(a), (c)] and polarization (0,1) [(b), (d)] located above an array of 53 inertial resonators with markedly inclined ligaments [(a), (b)] or within an homogeneous elastic medium [(c), (d)] at frequency $\omega d/c = 2$. The lensing effect in panel (a) and the neutral inclusion effect in panel (b) are noted: The array behaves as a negatively refracting slab lens for pressure waves and as an invisible slab (i.e., a perfectly matched layer) for shear waves. The computed image resolution is about a third of the wavelength (i.e., not subwavelength as is usually the case for a phononic crystal).

Focusing effects for an array of resonators. We show the focusing effect for arrays of inertial resonators. The focusing effect can be split into two categories: all-angle negative refraction whereby the array of IRs display an anomalous dispersion leading to a negative group velocity in certain directions (a phenomenon existing in phononic and photonic crystals; see, for example, Ref. 39), and genuine negative refraction whereby the focusing effect does not depend on the crystal lattice orientation (it occurs upon resonance of the IRs). The latter can be classified as a real acoustic metamaterial.

We analyze here the lensing effect achieved due to the anomalous dispersion corresponding to the acoustic bands, in a neighborhood of an intersection of the thick dashed line with the first band in Fig. 2. We consider a concentrated point force located near a finite array of resonators with inclined ligaments, and observe an image formed on the other side, according to the inverted Snell-Descartes laws of negative refraction in Fig. 5. Both cases, of vertical and horizontal point forces, are considered, which give different patterns of negative refraction.

V. CONCLUDING REMARKS AND PERSPECTIVES

We have proposed a type of structural element in order to design elastic metamaterials controlling the trajectory of in-plane coupled shear and pressure waves. The anisotropic heterogeneous elastic coating with each structural element can be modeled as a structural interface. Depending on the inclination of beams inside the coating, the overall behavior of the array of inertial resonators resembles that of a metamaterial (with a low-frequency stop band) which can be used in the design of antiseismic structures (thanks to low-frequency stop bands). In the periodic structure discussed here, the angle between the ligaments and the radial directions is a free control parameter, that enables one to fine tune the system to achieve band gaps and negative refraction within the required range of frequencies. There is a distinction between two different configurations of radial and nonradial elastic ligaments, with a substantial reduction of the resonance eigenfrequency in the degenerate case when the ligaments are radial. The coupling mechanism between the pressure state in the matrix and the shear stress induced by the rotation of the core resonator is fundamentally different from the one which occurs in a chiral lattice. The asymptotic formulas derived here for frequencies of standing waves and boundaries of stop bands are new and essential for an optimal design of a metamaterial structure. The microstructured system can also be tuned so that the localized rotational modes have frequencies within the Bragg stop band of an array of voids. Then a standard algorithm can be implemented to get trapped modes inside defects of a phononic crystal fiber and use the enhanced interactions of light and sound inside the defects to design fast optoacoustic switches.[37]

ACKNOWLEDGMENTS

Part of the reported work was performed under the support of the EU FP7 program under Contract No. PIAP-GA-2011-284544-PARM-2. D.B. gratefully acknowledges financial support from Grant No. PIAP-GA-2011-286110-INTERCER2, S.G. is thankful for EU funding through ERC Starting Grant ANAMORPHISM, and M.B. acknowledges the support of the EU FP7 under Contract No. PIEF-GA-2011-302357.

*Corresponding author: sebastien.guenneau@fresnel.fr

[1] N. A. Nicorovici, R. C. McPhedran, and G. W. Milton, Phys. Rev. B **49**, 8479 (1994).
[2] N. A. Nicorovici and G. W. Milton, Proc. R. Soc. London A **462**, 3027 (2006).
[3] V. G. Veselago, Sov. Phys. Usp. **10**, 509 (1968).
[4] J. B. Pendry, A. J. Holden, D. J. Robbins, and W. J. Stewart, IEEE Trans. Microwave Theory Tech. **47** (11), 2075 (1999).
[5] D. R. Smith, W. J. Padilla, D. C. Vier, S. C. Nemat-Nasser, and S. Schultz, Phys. Rev. Lett. **84** (18), 4184 (2000).
[6] A. B. Movchan and S. Guenneau, Phys. Rev. B **70**, 125116 (2004).
[7] S. Guenneau, A. B. Movchan, G. Petursson, and S. A. Ramakrishna, New J. Phys. **9**, 399 (2007).
[8] M. Brun, A. B. Movchan, and N. V. Movchan, Continuum Mech. Thermodyn. **22**, 663 (2010).
[9] M. Brun, S. Guenneau, A. B. Movchan, and D. Bigoni, J. Mech. Phys. Solids **58**, 1212 (2010).
[10] Z. Y. Liu, X. X. Zhang, Y. W. Mao, Y. Y. Zhu, Z. Y. Yang, C. T. Chan, and P. Sheng, Science **289**, 1734 (2000).
[11] J. Mei, Z. Liu, W. Wen, and P. Sheng, Phys. Rev. Lett. **96**, 024301 (2006).
[12] J. Li and C. T. Chan, Phys. Rev. E **70**, 055602 (2004).
[13] N. Fang, D. Xi, J. Xu, M. Ambati, W. Srituravanich, C. Sun, and X. Zhang, Nat. Mater. **5**, 452 (2004).
[14] G. W. Milton, M. Briane, and J. R. Willis, New J. Phys. **8**, 248 (2006).
[15] M. Brun, S. Guenneau, and A. B. Movchan, Appl. Phys. Lett. **94**, 061903 (2009).
[16] G. W. Milton, New J. Phys. **9**, 359 (2007).
[17] A. Norris, Proc. R. Soc. London A **464**, 2411 (2008).
[18] D. Bigoni, S. K. Serkov, M. Valentini, and A. B. Movchan, Int. J. Solids Struct. **35**, 3239 (1998).
[19] S. A. Cummer and D. Schurig, New J. Phys. **9**, 45 (2006).
[20] H. Chen and C. T. Chan, Appl. Phys. Lett. **91**, 183518 (2007).
[21] S. A. Cummer, B. I. Popa, D. Schurig, D. R. Smith, J. B. Pendry, M. Rahm, and A. Starr, Phys. Rev. Lett. **100**, 024301 (2008).
[22] M. Farhat, S. Enoch, S. Guenneau, and A. B. Movchan, Phys. Rev. Lett. **101**, 134501 (2008).
[23] X. Hu, Y. Shen, X. Liu, R. Fu, and J. Zi, Phys. Rev. E **69**, 030201 (2004).
[24] M. Farhat, S. Guenneau, S. Enoch, and A. B. Movchan, J. Comput. Appl. Math. **234**, 2011 (2010).
[25] M. Farhat, S. Guenneau, S. Enoch, and A. B. Movchan, Phys. Rev. E **80**, 046309 (2009).
[26] S. Yang, J. H. Page, Z. Liu, M. L. Cowan, C. T. Chan, and P. Sheng, Phys. Rev. Lett. **93**, 024301 (2004).
[27] X. Zhou and G. Hu, Phys. Rev. B **79**, 195109 (2009).
[28] J. Li, L. Fok, X. Yin, G. Bartal, and X. Zhang, Nat. Mater. **8**, 931 (2009).
[29] S. H. Lee, C. M. Park, Y. M. Seo, Z. G. Wang, and C. K. Kim, Phys. Rev. Lett. **104**, 054301 (2010).
[30] Y. Lai, Y. Wu, P. Sheng, and Z. Q. Zhang, Nat. Mater. **10**, 620 (2011).
[31] M. Farhat, S. Guenneau, S. Enoch, A. B. Movchan, and G. Petursson, Appl. Phys. Lett. **96**, 081909 (2010).
[32] C. P. Chen and R. S. Lakes, Cellular Polymers **8**, 343 (1989).
[33] D. Prall and R. S. Lakes, Int. J. Mech. Sci. **39**, 305 (1996).
[34] K. Wojciechowski, Phys. Lett. A **137**, 60 (1989).
[35] A. Spadoni and M. Ruzzene, J. Mech. Phys. Solids **60**, 156 (2012).
[36] X. N. Liu, G. L. Huang, and G. K. Hua, J. Mech. Phys. Solids **60**, 1907 (2012).
[37] P. St. Russell, E. Marin, A. Diez, S. Guenneau, and A. B. Movchan, Opt. Express **11** (20), 2555 (2003).
[38] S. Guenneau, A. Movchan, C. Poulton, and A. Nicolet, Q. J. Mech. Appl. Math. **57**, 407 (2004).
[39] C. Luo, S. G. Johnson, J. D. Joannopoulos, and J. B. Pendry, Phys. Rev. B **65**, 201104 (2002).